# Progressive Curriculum Learning with Scale-Enhanced U-Net for Continuous Airway Segmentation

Bingyu Yang, Qingyao Tian, Huai Liao, Xinyan Huang, Jinlin Wu, Jingdi Hu and Hongbin Liu

Abstract—Continuous and accurate segmentation of airways in chest CT images is essential for preoperative planning and real-time bronchoscopy navigation. Despite advances in deep learning for medical image segmentation, maintaining airway continuity remains a challenge, particularly due to intra-class imbalance between large and small branches and blurred CT scan details. To address these challenges, we propose a progressive curriculum learning pipeline and a Scale-Enhanced U-Net (SE-UNet) to enhance segmentation continuity. Specifically, our progressive curriculum learning pipeline consists of three stages: extracting main airways, identifying small airways, and repairing discontinuities. The cropping sampling strategy in each stage reduces feature interference between airways of different scales, effectively addressing the challenge of intra-class imbalance. In the third training stage, we present an Adaptive Topology-Responsive Loss (ATRL) to guide the network to focus on airway continuity. The progressive training pipeline shares the same SE-UNet, integrating multi-scale inputs and Detail Information Enhancers (DIEs) to enhance information flow and effectively capture the intricate details of small airways. Additionally, we propose a robust airway tree parsing method and hierarchical evaluation metrics to provide more clinically relevant and precise analysis. Experiments on both in-house and public datasets demonstrate that our method outperforms existing approaches, significantly improving the accuracy of small airways and the completeness of the airway tree. The code will be released upon publication.

#### I. INTRODUCTION

Accurate airway segmentation and reconstruction from CT images are crucial for preoperative planning, real-time navigation, and detecting peripheral pulmonary lesions [1]. In clinical practice, only the largest connected component of the segmented airway is used for bronchoscopic localization and navigation to provide a clear and accessible path. This makes continuity in segmentation critical. However, manual segmentation of complex pulmonary airways in CT images is time-consuming and error-prone. Therefore, there is an

Bingyu Yang and Qingyao Tian are with State Key Laboratory of Multimodal Artificial Intelligence Systems, Institute of Automation, Chinese Academy of Sciences, Beijing 100190, China, and also with the School of Artificial Intelligence, University of Chinese Academy of Sciences, Beijing 100049, China.

Huai Liao, M.D., Xinyan Huang, M.D. and Jingdi Hu, M.D. are with Department of Pulmonary and Critical Care Medicine, The First Affiliated Hospital of Sun Yat-sen University, Guangzhou, Guangdong Province, P.R. China.

Jinlin Wu is with Institute of Automation, Chinese Academy of Sciences, Beijing, 100190, China, and also with Centre of AI and Robotics, Hong Kong Institute of Science & Innovation, Chinese Academy of Sciences.

Corresponding author: Hongbin Liu is with Institute of Automation, Chinese Academy of Sciences, and with Centre of AI and Robotics, Hong Kong Institute of Science & Innovation, Chinese Academy of Sciences. He is also affiliated with the School of Biomedical Engineering and Imaging Sciences, King's College London, UK. (e-mail: liuhongbin@ia.ac.cn).

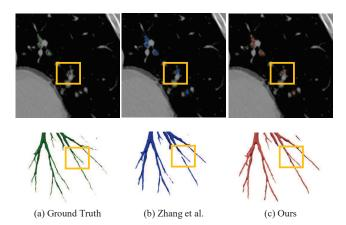


Fig. 1. Example of airway discontinuity. (a) Green mask: ground truth. (b) Blue mask: prediction based on Zhang et al. [8]. (c) Red mask: prediction based on our method. Blurry airway walls lead to discontinuities, which were not effectively addressed by [8] (yellow box).

urgent need for automated technologies to achieve accurate and continuous airway segmentation.

Recent deep learning methods [2]–[9] have made significant strides in improving segmentation accuracy compared to traditional techniques [10]–[13]. However, two major challenges remain unaddressed towards achieving continuous airway segmentation: 1) *intra-class imbalance* between major and smaller branches, and 2) *blurred details in CT imaging*. As a result, despite good overlap with ground truth, existing methods often produce fragmented segments, restricting their clinical applicability [5]–[8].

Intra-class Imbalance. The airway tree has a complex branching structure with significant volume and morphological differences between major and smaller airways, termed intra-class imbalance. Zheng et al. [6] showed that this imbalance causes smaller airway features to be overshadowed by major airways during training, making it difficult for models to focus on smaller structures. Despite their novel supervision approach and distance-based loss function, the issue of airway breakage is not addressed, and missed detections in peripheral small airways persist, leading to airway discontinuities.

Blurred Details in CT Imaging. In CT imaging, distal small airways are limited by resolution, noise, and motion blur, often showing low signal-to-noise ratios and blurred details. Fine branches and edge information are easily lost during downsampling, making it hard to restore their integrity during upsampling and causing airway discontinuities. The Connectivity-Aware Surrogate (CAS) and Local-

Sensitive Distance (LSD) modules proposed by Zhang et al. [8] represent the best current approach to addressing airway discontinuities, but they still fail to handle certain blurred airway walls (Fig. 1).

To address intra-class imbalance and reduce interference in feature learning, we propose a progressive curriculum learning pipeline for airway segmentation, inspired by curriculum learning [14]. We also present a Scale-Enhanced U-Net (SE-UNet) to improve the extraction of airway features across multiple scales, enhancing segmentation accuracy. Additionally, we present hierarchical evaluation metrics to assess performance, emphasizing segmentation continuity at different scales using robust airway tree parsing method.

Motivated by the advancements of curriculum learning in improving segmentation performance by learning from easy to complex tasks [15]–[17], we propose a progressive curriculum learning pipeline to address intra-class imbalance. This pipeline consists of three stages: extracting main airways, identifying small airways, and repairing discontinuities. To effectively sample training data at each stage, we design three crop sampling strategies (Random Crop, Hard-mining Crop, and Breakage Crop) to mine curriculum samples. A dynamic training scheduler automatically adjusts the input ratio of these samples based on stage-wise performance. To further enhance segmentation continuity, we propose an Adaptive Topology-Responsive Loss (ATRL) to emphasize overlap between predicted and ground-truth centerlines, guiding the network to segment airway with enhanced continuity.

To address discontinuities caused by blurred details in CT imaging, we propose Scale-Enhanced U-Net (SE-UNet). SE-UNet captures airway features at multiple scales, enhancing contextual and edge detail restoration. It uses pyramid pooling on the input image and integrates multi-scale inputs with feature information via residual connections, improving gradient propagation and reducing vanishing gradients. To further enrich critical information, we propose Detail Information Enhancers (DIEs), improving multi-scale feature capture and edge detail recovery.

Existing metrics overlook the evaluation of continuity of segmentation. Moreover, they suffer from bias caused by class imbalance, as larger airways dominate metrics, obscuring deficiencies in small airway segmentation. To accurately evaluate segmentation performance, we present hierarchical evaluation metrics that assess topological completeness at different airway levels. The core is an optimized airway tree parsing algorithm that addresses false branches and handles individual differences by smoothing centerlines, pruning, and merging branches. Extensive experiments on public (499 cases) and in-house datasets (55 cases) demonstrate that our method significantly improves topological completeness compared to state-of-the-art methods, with notable advantages in small airway extraction.

In summary, our contributions are as follows:

 A progressive curriculum learning pipeline integrated with Adaptive Topology-Responsive Loss (ATRL) is proposed to address intra-class imbalance, enhancing

- continuous airway segmentation.
- We propose the Scale-Enhanced U-Net (SE-UNet) with Detail Information Enhancer (DIE) to reduce information loss during downsampling, reducing the impact of blurred details in CT imaging.
- Hierarchical evaluation metrics are presented to accurately assess segmentation completeness at different scales through a robust airway tree parsing method.
- Experiments on both public and in-house datasets demonstrate that our method has significant advantages in small airway extraction and airway continuity.

## II. RELATED WORKS

Airway segmentation is crucial for the diagnosis and surgical planning of pulmonary diseases. Traditional methods [10]–[13], [19] have been applied. The EXACT 09 challenge [20] proposed 15 segmentation algorithms. However, the results indicated that these methods are ineffective in extracting small airways.

In recent years, advancements in deep learning have significantly improved the performance of automated airway segmentation [2]–[8]. Juarez et al. [2] proposing a 3D U-Net that improved feature representation but struggled with small airway detection. This limitation arose due to CT noise, which caused the features of distal small airways to be blurred.

To enhance feature extraction, Qin et al. [5] added feature recalibration and attention distillation modules, and Selvan et al. [4] treated the problem as graph refinement. However, the size differences between airway tree branches continue to pose a challenge for feature extraction. Zheng et al. [6] defined this problem as intra-class imbalance, where large airway features dominate the learning process, leading to missed detection of peripheral small airways and resulting in airway discontinuity.

To address intra-class imbalance and airway discontinuity issues, Qin et al. [3] proposed AirwayNet to enhance voxel connectivity. Zheng et al. [6] introduced the General Union Loss (GUL) to alleviate this problem. The distance-based loss function improved the model's focus and learning of the airway centerline but did not directly solve the airway discontinuity problem. Zhang et al. [8] introduced Connectivity-Aware Surrogate (CAS) and Local-Sensitive Distance (LSD) modules, which improved connectivity but led to oversegmentation issues.

In this work, we propose a progressive curriculum learning pipeline based on curriculum learning that effectively addresses the intra-class imbalance issue, and a SE-UNet which enhances multi-scale information.

#### III. METHOD

In the following section, we present the progressive curriculum learning pipeline (§III.A) and SE-UNet (§III.B), which enhances information flow and segmentation details. Additionally, we propose hierarchical evaluation metrics to provide fair evaluation emphasizing continuity (§III.C).

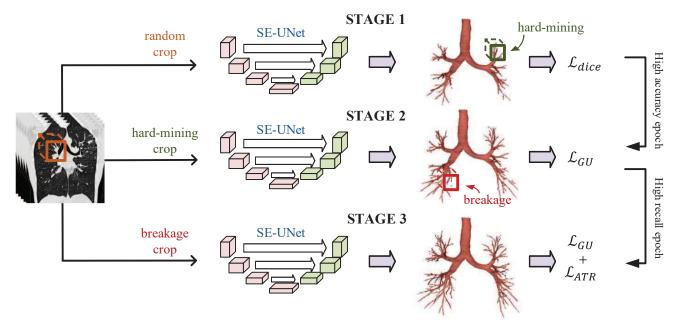


Fig. 2. Overview of the proposed progressive curriculum learning pipeline for airway segmentation. In "Stage 1", the network is trained utilizing the Dice Loss [18]. The epoch with the highest accuracy from the "Stage 1" forms the basis for the hard-mining strategy employed in the "Stage 2". This stage focuses on learning to detect the challenging airways with GUL [6]. Building upon the predictions with the highest recall from "Stage 2", the "Stage 3" introduces ATRL to enhance the length of the airway tree. Ultimately, the optimal model is selected for segmentation testing.

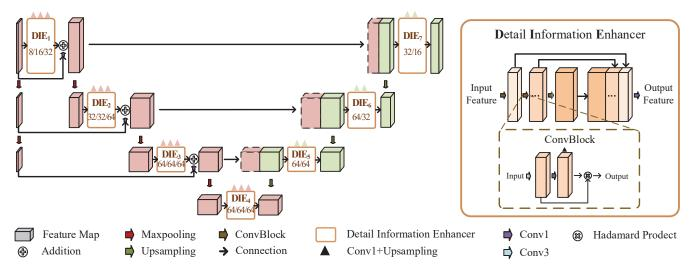


Fig. 3. The SE-UNet architecture in proposed method. "DIE $_1$  8/16/32" refers to the output channels of the three ConvBlocks in DIE $_1$  are 8, 16 and 32. The detailed structure of DIE is shown in the orange box.

## A. Progressive curriculum learning pipeline

Due to the large volume of 3D lung CT data and GPU memory limitations, airway segmentation networks are trained using sampling patches as inputs [2], [7]. When patches contain both large and small airways, intra-class imbalance causes loss gradients to be dominated by large airways, exacerbating gradient erosion in small airways [6]. To address this, we design a progressive curriculum learning pipeline to train the network and minimize interference during feature learning (Fig. 2). The pipeline consists of three stages: extracting main airways, identifying small airways, and repairing discontinuities. We develop three crop sam-

pling strategies to effectively mine curriculum samples, and the training scheduler dynamically adjusts the input ratio of these samples based on the performance of each stage. The specific design and function of each stage are as follows:

**Stage 1:** The network is trained on airway patches using Random Crop Sampling to learn basic tubular features and achieves rapid convergence under the supervision of Dice loss [18]:

$$\mathcal{L}_1 = \mathcal{L}_{dice} = 1 - \frac{2\sum_{i=1}^{N} p_i g_i}{\sum_{i=1}^{N} (p_i + g_i)},$$
 (1)

where N is the total number of voxels,  $p_i$  is the i-th voxel' prediction and  $g_i$  is the ground truth.

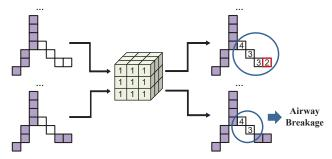


Fig. 4. Explanation of identifying airway breakages. Here shows an airway skeleton segment, with purple points representing successful predictions and white points indicating failures. A 3×3×3 all-ones convolution kernel is applied to the white points to count their neighbors. If no point on a challenging airway segment has a single neighbor, it is identified as a breakage.

**Stage 2:** Hard-mining Crop Sampling is introduced to select unextracted airway skeleton points from Stage 1 predictions to generate patches. The training scheduler dynamically adjusts the weights based on the quantities of random and hard-mining sampling patches. This stage is supervised by General Union Loss (GUL) [6] to address potential intraclass imbalance and enhance the extraction of peripheral small airways:

$$\mathcal{L}_{2} = \mathcal{L}_{GU} = 1 - \frac{\sum_{i=1}^{N} w_{i} p_{i}^{\gamma} g_{i}}{\sum_{i=1}^{N} w_{i} (\alpha p_{i} + \beta g_{i})},$$
(2)

where Local-imbalance-based Weight  $w_l$  [21] adjusts airway voxel weights by branch size. According to [6], we choose  $\gamma = 0.7$ ,  $\alpha = 0.2$ ,  $\beta = 0.8$ .

**Stage 3:** The most challenging aspect is optimizing airway discontinuities heavily influenced by CT noise. We propose Breakage Crop Sampling to isolate discontinuity-related segments using a 3×3×3 all-ones convolution kernel on challenging airway skeleton points from Stage 2 (as shown in Fig. 4). Similarly, the training scheduler dynamically adjusts the ratio of random, hard-mining, and breakage sampling patches. In this stage, we propose a Adaptive Topology-Responsive Loss (ATRL), as defined in (3). This loss function penalizes voxels that are difficult to detect within the airway skeleton, placing greater emphasis on the continuity of the airway.

$$\mathcal{L}_{ATR} = 1 - \frac{\sum_{i=1}^{C} w_i p_i g_i}{\sum_{i=1}^{C} w_i (p_i + g_i)},$$
 (3)

where C is the number of voxels on the airway centerline. To focus on hard-to-segment small airways,  $w_i$  is is written as follow:

$$w_i = w_l + w_c, \tag{4}$$

where Centerline-distance-based Weight  $w_c$  provides increased attention to points near the difficult-to-segment airway centerline to maintain branch continuity, with additional weight assigned to voxels that contribute to breakage:

$$w_c = \left(1 - \frac{d_i}{d_{max}}\right)^2 + \eta \cdot min(1 - d_i, K), \qquad (5)$$

where  $d_i$  is the shortest distance from the i-th voxel to the centerline,  $d_{max}$  is its maximum value.  $\eta$  indicates whether the i-th voxel induces breakage ( $\eta$ =1 if it does, otherwise  $\eta$ =0). K is a hyper-parameter set to 2 to prevent  $w_c$  from becoming too large.

In the third stage of training, the hybrid loss function is:

$$\mathcal{L}_3 = \mathcal{L}_{GU} + \mathcal{L}_{ATR}.\tag{6}$$

# B. Scale-Enhanced U-Net

The pulmonary airway structure is complex, consisting of multi-scale airway branches that pose significant challenges in feature extraction due to imaging noise and intra-class imbalance. To address these issues, we propose a Scale-Enhanced U-Net (SE-UNet). This architecture achieves hierarchical residual nesting through the use of multi-scale inputs and Detail Information Enhancers (DIEs). The overall network structure is depicted in Fig. 3. Specifically, the 3D patches input to the network are pyramid-pooled into three resolutions, with residuals computed using a 1×1×1 convolution layer and the output features from the residual multi-scale encoder at each stage. The SE-UNet effectively captures and integrates multi-scale airway information during the encoding phase, enhancing its ability to model complex airway structures.

The SE-UNet comprises a total of 7 Detail Information Enhancers (DIEs), divided into an encoding group (DIE 1-4) and a decoding group (DIE 5-7). In encoder, the features extracted by the i-th layer are obtained by:

$$F_{en_i} = \text{Conv1}(\text{Maxpool}_i(F_{in})) \oplus F_{DIE_i},$$
 (7)

where Conv1 is  $1\times1\times1$  convolution,  $\operatorname{Maxpool}_i$  represents the maxpooling at the i-th depth level and  $\oplus$  denotes addition.  $F_{in}$  is the input feature and  $F_{DIE_i}$  is the output of the DIE at the i-th encoder layer.

Similarly, the features recovered by the i-th decoding layer are obtained by:

$$F_{de_i} = F_{DIE_i}. (8)$$

Group supervision has been shown to effectively alleviate inter-class imbalance [6], so it is introduced for supervising the encoding and decoding groups in SE-UNet.

**Detail Information Enhancer:** The DIE is an Inception-like architecture [22] that integrates multi-scale features extracted by convolutional layers of varying depths and enhances details, as shown in the orange box of Fig. 3. Each DIE consists of n ConvBlocks, "DIE $_i$   $c_1/\ldots/c_n$ " refers to the output channels of n ConvBlocks in DIE $_i$ . Each ConvBlock includes convolution layers, an instance normalization layer and a ReLU layer. It outputs features to the next block  $f_{i,j}$  while generating an additional path through the upsampling layer, forming a group feature pyramid that is used for group supervision [6]. The output of the i-th DIE to the next module  $F_{DIE_i}$  is calculated as:

$$F_{DIE_i} = \text{Conv1}(\text{Cat}(f_{i,1}, f_{i,2}, \dots, f_{i,n})),$$
 (9)

where Cat denotes concatenation,  $f_{i,j}$  represents the feature of the j-th ConvBlock in the i-th DIE. n is the total number

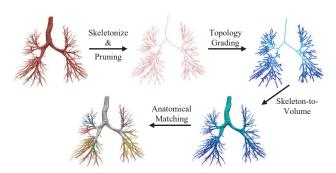


Fig. 5. A qualitative example illustrating the topological analysis process of airway tree.

of blocks in this DIE (3 in the encoder and 2 in the decoder).

$$f_{0,j} = \text{RELU}(\text{IN}(\text{Conv3}(f_{i,j-1}))), \tag{10}$$

$$f_{i,j} = \text{Sigmoid}(\text{Conv1}(f_{0,j})) \odot f_{0,j},$$
 (11)

where  $f_{0,j}$  is a intermediate result, IN denotes instance normalization, Conv3 is  $3\times3\times3$  convolution,  $f_{i,j-1}$  represents the output of the previous block.  $\odot$  is Hadamard product.

### C. Hierarchical Evaluation

Current airway segmentation research uses Tree length Detected rate(TD) and Branch Detected rate(BD) to assess airway completeness, Dice Similarity Coefficient(DSC) and Precision(Pre) to measure accuracy [23]. However, these metrics are limited by false branches and intra-class imbalance, masking deficiencies in small airway segmentation. Thus, we propose hierarchical evaluation metrics based on Robust Airway Tree Parsing (Fig. 5) to evaluate topological completeness at different airway levels.

Robust Airway Tree Parsing: Existing methods include skeleton-based analysis [24] and deep learning-based classification [25]. However, the former often generates inaccurate skeletons, while the latter misses high-order branches. We propose a robust airway tree parsing pipeline that includes Skeletonization and Parsing, Pruning, Topology Grading, and Anatomical Matching. (a) Skeletonization and Parsing: Traverse the extracted skeleton to identify branch points and explore along the skeleton line from each branch point until the airway end or the next branch point is reached. Record parent-child relationships to complete skeleton parsing. (b) Pruning: Smooth the main airway segments, remove peripheral short segments, and merge single-segment parent branches to accurately divide airway branches. (c) Topology Grading: Recursively number branch points along the skeleton. (d) Anatomical Matching: Align the original numbering with anatomical grades based on hierarchical relationships and airway angles, considering common branch omissions and individual differences to achieve stable airway tree parsing.

**Evaluation Metrics:** In addition to the commonly used metrics (TD, BD, DSC, and Pre), we propose hierarchical evaluation metrics to mitigate biases caused by the intraclass imbalance. Following the anatomical labeling in [26],

we define two levels: Large airways = trachea + main bronchi + lobar bronchus (gray airways after anatomy matching in Fig. 5) and Small airways = segmental airways (colored airways). The hierarchical evaluation metrics for airway completeness are formulated as follows:

$$TD_{L(S)} = \frac{\hat{T}_{L(S)}}{T_{L(S)}},$$
 (12)

$$BD_{L(S)} = \frac{\hat{B}_{L(S)}}{B_{L(S)}},$$
 (13)

where  $\hat{T}_{L(S)}$  refers to the total detected branch length for Large (Small) airways, while  $T_{L(S)}$  represents the length of the these branches in the ground truth.  $\hat{B}_{L(S)}$  denotes the number of correctly detected Large (Small) branches, and  $B_{L(S)}$  is the ground truth.

## IV. EXPERIMENT

## A. Dataset

We evaluate our method on two datasets: in-house dataset used for training, assessment, and ablation studies; the ATM'22 challenge dataset [23] for fair comparative testing<sup>1</sup>.

ATM'22 challenge dataset: This dataset provides 499 CT scans: 299 for training, 50 for validation, and 150 for testing [3], [6], [27], [28], sourced from EXACT'09 [20], LIDC-IDRI [29], and Shanghai Chest Hospital. Three radiologists with over five years of experience meticulously annotated the CT images. We trained our model on the train dataset, with test results evaluated by the challenge organizers.

**In-house dataset:** We collected and annotated 55 CT scans from The First Affiliated Hospital of Sun Yat-sen University, including samples from healthy subjects as well as patients with mild COPD and ILD. Each scan contains 256 to 612 slices, with spatial resolution ranging from 0.598 to 0.879 mm and slice thickness from 0.625 to 1.000 mm. The scans were split into training (35), validation (10), and test sets (10). Initial segmentation was done using models [6], followed by detailed annotations by three pulmonologists, finalized through majority voting.

# B. Implementation Details

Preprocessing involves truncating CT voxel intensities to [-1000,500] and [-1024,1024], followed by normalization to [0,1]. The network is trained using  $128\times128\times128$  CT patches as input. The optimizer used is AdamW with a batch size of 2 and a learning rate of 0.0001. The training epochs for the three stages are set to 100, 50, and 50, respectively. For post-processing, Dual Threshold Iteration (DTI) [30] is employed to convert the probability map to a binary mask, followed by morphological hole filling and extraction of the largest connected component. Thresholds in DTI are set at  $T_h = 0.5$  and  $T_l = 0.35$ . The framework is implemented using PyTorch 2.0.0 and both training and inference are conducted on a single NVIDIA RTX 4090 GPU. In inference, our approach can achieve an average segmentation time of 73 ms per  $128\times128\times128$  CT patch.

<sup>1</sup>https://atm22.grand-challenge.org/

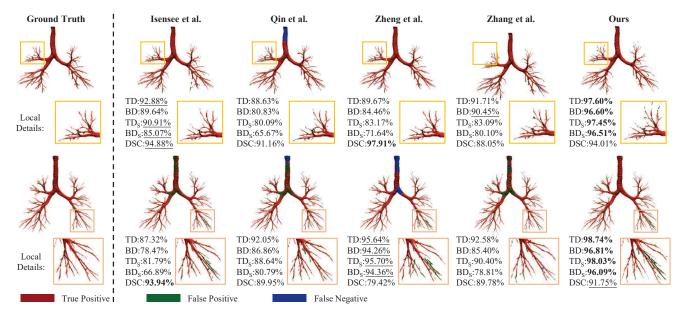


Fig. 6. Visualization of the segmentation results of the our approach and other SOTA methods. Red, green, and blue represent correct airways(true positive), airway leakages(false positive) and missing airways(false negative), respectively. Best viewed in color and magnified.

TABLE I

COMPARISON ON ATM22 TEST DATASET. THE **BEST** AND <u>SECOND-BEST</u>

ARE HIGHLIGHTED.

Team	TD(%)	BD(%)	DSC(%)	Pre(%)	wMS
neu204 [31]	90.974	86.670	94.056	93.027	90.710
	$\pm 10.409$	$\pm 13.087$	±8.021	$\pm 8.410$	
YangLab [7]	94.512	91.920	94.800	94.707	93.831
	±8.598	±9.435	±7.925	±8.302	
deeptree_damo [9]	97.853	97.129	92.819	87.928	94.644
	±2.275	±3.411	±2.191	$\pm 4.181$	
timi	95.919	94.729	93.910	93.553	94.687
	±5.234	±6.385	±3.682	$\pm 3.420$	
Ours	96.425	95.479	93.827	91.781	94.693
	±3.156	±4.313	±1.897	±4.110	

## V. RESULTS

## A. Comparison Results

The ATM'22 challenge organizers conducted a quantitative analysis of our method's performance on a hidden test set. Table I compares our test results with those of the top four teams in the competition, ranked by weighted mean score(wMS). To assess the sensitivity of different algorithms to airway continuity, we emphasize the geometric shape of airway predictions through the weighted average score. The weighted mean score(wMS) is calculated as 30% TD, 30% BD, 20% DSC and 20% Precision. Our method achieved the highest weighted average score of 94.693. Notably, our method outperformed timi in TD (96.425%) and BD (95.479%) scores. Our precision score (91.781%) was slightly lower than other metrics. After a careful analysis of the training and validation sets provided by the organizers by medical experts, it was found that some peripheral branches in the dataset were not fully annotated. We speculate that this might be because our method successfully detected

TABLE II

COMPARISON ON IN-HOUSE DATASET.\* DENOTES RESULTS FROM AN OPEN-SOURCE MODULE (WITH TRAINED WEIGHTS). † INDICATES THE RESULTS FROM MODULES TRAINED USING OPEN-SOURCE CODES.

Method	TD(%)	BD(%)	DSC(%)	Pre(%)
Isensee et al. [32] <sup>†</sup>	82.453	72.019	93.132	92.931
	±11.817	±14.990	$\pm 4.065$	$\pm 7.323$
Qin et al. [33]*	86.300	81.783	88.755	89.870
	±11.571	±15.655	±3.373	±4.340
Zheng et al. [6]*	89.296	84.739	91.052	90.814
	±2.872	±4.389	±1.098	±6.769
Zhang et al. [8]*	90.434	85.418	88.803	81.407
	±3.060	$\pm 6.807$	$\pm 0.760$	±1.154
Ours	92.784	90.040	91.488	87.190
	±3.665	±5.7327	±1.230	±2.322
	$TD_L(\%)$	$BD_L(\%)$	$TD_S(\%)$	$BD_S(\%)$
Isensee et al. [32] <sup>†</sup>	87.324	82.775	70.425	59.375
Qin et al. [33]*	90.820	88.536	70.721	61.924
Zheng et al. [6]*	91.862	91.457	75.545	65.407
Zhang et al. [8]*	93.350	91.493	80.903	71.710
Ours	94.857	92.452	90.534	74.532

these unannotated peripheral branches on the hidden test set, thereby affecting the precision metric. As illustrated in Fig. 6, our algorithm exhibits a reliable capacity for detecting more peripheral airways. Compared to other teams, our TD and BD scores were 1.9% and 3.6% higher than the YangLab team [7], and 5.5% and 8.8% higher than the neu204 team [31]. The deeptree\_damo team [9], in their pursuit of higher airway completeness, sacrificed precision, resulting in the lowest DSC (92.819%) and Precision scores (87.928%). Overall, our method strikes an excellent balance between airway accuracy and completeness, achieving the highest mean score.

Based on the proposed robust airway tree parsing, the evaluation results on our in-house dataset are shown in

TABLE III

ABLATION STUDY ON IN-HOUSE DATASET. 'DIE': DETAIL INFORMATION ENHANCER; 'DIE\_EN'OR 'DIE\_DE': DIE IN THE ENCODER OR DECODER; 'ATRL': ADAPTIVE TOPOLOGY-RESPONSIVE LOSS.

Method	TD(%)	BD(%)	DSC(%)	Pre(%)
Ours w/o DIE	88.358	82.400	91.868	87.676
	±5.787	±9.767	±0.530	$\pm 1.105$
Ours w/o DIE_en	89.066	83.396	93.038	89.563
	±5.363	±8.110	±1.025	±2.013
Ours w/o DIE_de	89.529	83.850	92.918	89.121
	±5.940	±8.718	$\pm 0.472$	±1.091
Ours w/o ATRL	90.118	84.758	93.244	89.502
	±4.674	$\pm 7.846$	$\pm 0.534$	$\pm 1.207$
Ours_Stage1	71.922	60.286	93.118	91.593
	±7.993	±8.419	$\pm 0.867$	$\pm 0.941$
Ours_Stage1+2	88.068	81.550	92.908	89.309
	±5.734	±8.514	$\pm 0.943$	±1.752
Ours	92.784	90.040	91.488	87.190
	±3,665	$\pm 5.733$	±1.230	±2.322

Table II. Our method is compared with other state-of-theart methods from the past five years, achieving the highest TD (92.784%), BD (90.040%) and the second-highest DSC at 91.488%. The nnUNet by Isensee et al. [32] achieved the highest DSC (93.132%) and Precision (92.931%), but it does not specifically address airway segmentation challenges, resulting in poorer airway continuity. Qin et al. [33] combined a 3D UNet with an attention distillation module to improve the detection of peripheral small airways, achieving TD (86.300%) and BD (81.783%). However, their method did not effectively address the issue of class imbalance. Zheng et al. [6] introduced the GUL and a new supervision to tackle class imbalance. However, GUL did not directly penalize airway discontinuities, resulting in TD (89.296%) and BD (84.739%). Zhang et al. [8] proposed a Connectivity-Aware Surrogate (CAS) module to improve airway continuity but introduced potential over-segmentation issues. Although their method achieved the second-highest TD (90.434%) and BD (85.418%), it had the lowest Pre at 81.407%. To compare the completeness across different airway branch sizes, the lower part of Table II shows the tree length and branch detection results for large airways (trachea, main bronchi, lobar bronchus) and small airways (segmental airways), denoted as  $TD_L$ ,  $BD_L$  and  $TD_S$ ,  $BD_S$ . Fig. 6 visualizes the segmentation results of our method and other SOTA methods, further demonstrating our significant advantages in small airway segmentation and airway tree continuity.

### B. Ablation Studies

In our in-house dataset, we conducted a detailed analysis of our method's components: (a) the effectiveness of the Detail Information Enhancer (DIE); (b) the impact of the Adaptive Topology-Responsive Loss (ATRL); and (c) the importance of the second and third stages in the progressive curriculum learning pipeline. Table III presents the quantitative results of this ablation study.

Firstly, we evaluated the impact of removing the Detail Information Enhancers (DIEs). Omitting DIEs (Ours w/o

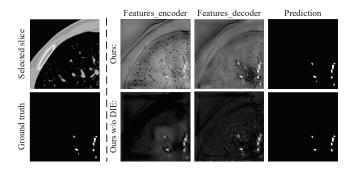


Fig. 7. The impact of the DIE. The feature maps from the encoder and decoder are shown on the right.

DIE) slightly affected the DSC and Pre but significantly reduced TD and BD by 4.426% and 7.640%, respectively. This indicates that DIEs play a crucial role in maintaining airway continuity, especially when segmenting the blurred airways in CT images (as shown in Fig. 7). Specifically, the absence of multi-scale inputs and DIEs in the encoding stage (Ours w/o DIE\_en) notably impaired gradient propagation for small airways, thereby affecting the integrity of airway prediction. In contrast, DIEs in the decoder successfully restored the blurred features, significantly improving tree length.

Secondly, the effectiveness of ATRL was explored. The model incorporating ATRL showed improvements in TD (2.666%) and BD (5.282%), confirming that ATRL effectively encourages the network to focus on the airway breakages, thereby enhancing the segmentation accuracy.

Lastly, we compared the network trained through all three stages with those trained through only the first stage or the first two stages, with the results shown in the last three rows of Table III. The second and third stages improved TD and BD by 16.146% and 4.716%, and by 21.264% and 8.490%, respectively. It shows that the second stage enhances peripheral airway detection, while the third stage further improves airway continuity by addressing discontinuities.

### VI. CONCLUSIONS

In this study, we propose a progressive curriculum learning pipeline and a Scale-Enhanced U-Net (SE-UNet), achieving accurate and continuous airway segmentation. The progressive curriculum learning pipeline reduces feature interference between different scales and alleviates intra-class imbalance. Additionally, the Adaptive Topology-Responsive Loss (ATRL) proposed in the third stage further optimizes airway continuity. All three training stages share the same Scale-Enhanced U-Net (SE-UNet), which captures the blurred details of small airways through multi-scale inputs and Detail Information Enhancers (DIEs). Experiments demonstrate that our method outperforms existing approaches in small airway detection and airway tree completeness, providing more reliable segmentation results for preoperative planning and real-time bronchoscopy navigation.

#### REFERENCES

- T. Ishiwata, A. Gregor, T. Inage, and K. Yasufuku, "Bronchoscopic navigation and tissue diagnosis," *General thoracic and cardiovascular* surgery, vol. 68, pp. 672–678, 2020.
- [2] A. Garcia-Uceda Juarez, H. A. Tiddens, and M. de Bruijne, "Automatic airway segmentation in chest CT using convolutional neural networks," in *Image Analysis for Moving Organ, Breast, and Thoracic Images*. Springer, 2018, pp. 238–250.
- [3] Y. Qin, M. Chen, H. Zheng, Y. Gu, M. Shen, J. Yang, X. Huang, Y.-M. Zhu, and G.-Z. Yang, "AirwayNet: a voxel-connectivity aware approach for accurate airway segmentation using convolutional neural networks," in *MICCAI*. Springer, 2019, pp. 212–220.
- [4] R. Selvan, T. Kipf, M. Welling, A. G.-U. Juarez, J. H. Pedersen, J. Petersen, and M. de Bruijne, "Graph refinement based airway extraction using mean-field networks and graph neural networks," *Medical image analysis*, vol. 64, p. 101751, 2020.
- [5] Y. Qin, H. Zheng, Y. Gu, X. Huang, J. Yang, L. Wang, and Y.-M. Zhu, "Learning bronchiole-sensitive airway segmentation CNNs by feature recalibration and attention distillation," in *MICCAI*. Springer, 2020, pp. 221–231.
- [6] H. Zheng, Y. Qin, Y. Gu, F. Xie, J. Yang, J. Sun, and G.-Z. Yang, "Alleviating class-wise gradient imbalance for pulmonary airway segmentation," *IEEE transactions on medical imaging*, vol. 40, no. 9, pp. 2452–2462, 2021.
- [7] Y. Nan, J. Del Ser, Z. Tang, P. Tang, X. Xing, Y. Fang, F. Herrera, W. Pedrycz, S. Walsh, and G. Yang, "Fuzzy attention neural network to tackle discontinuity in airway segmentation," *IEEE Transactions on Neural Networks and Learning Systems*, 2023.
- [8] M. Zhang and Y. Gu, "Towards connectivity-aware pulmonary airway segmentation," *IEEE Journal of Biomedical and Health Informatics*, 2023.
- [9] P. Wang, D. Guo, D. Zheng, M. Zhang, H. Yu, X. Sun, J. Ge, Y. Gu, L. Lu, X. Ye, et al., "Accurate airway tree segmentation in CT scans via anatomy-aware multi-class segmentation and topologyguided iterative learning," *IEEE Transactions on Medical Imaging*, 2024.
- [10] D. Aykac, E. A. Hoffman, G. McLennan, and J. M. Reinhardt, "Segmentation and analysis of the human airway tree from threedimensional X-ray CT images," *IEEE transactions on medical imag*ing, vol. 22, no. 8, pp. 940–950, 2003.
- [11] J. Tschirren, E. A. Hoffman, G. McLennan, and M. Sonka, "Intrathoracic airway trees: segmentation and airway morphology analysis from low-dose CT scans," *IEEE transactions on medical imaging*, vol. 24, no. 12, pp. 1529–1539, 2005.
- [12] A. P. Kiraly, W. E. Higgins, G. McLennan, E. A. Hoffman, and J. M. Reinhardt, "Three-dimensional human airway segmentation methods for clinical virtual bronchoscopy," *Academic radiology*, vol. 9, no. 10, pp. 1153–1168, 2002.
- [13] S. Born, D. Iwamaru, M. Pfeifle, and D. Bartz, "Three-step segmentation of the lower airways with advanced leakage-control," in *Proc.* of Second International Workshop on Pulmonary Image Analysis. Citeseer, 2009, pp. 239–249.
- [14] Y. Bengio, J. Louradour, R. Collobert, and J. Weston, "Curriculum learning," in *ICML*, 2009, pp. 41–48.
- [15] Z. Liu, V. Manh, X. Yang, X. Huang, K. Lekadir, V. Campello, N. Ravikumar, A. F. Frangi, and D. Ni, "Style curriculum learning for robust medical image segmentation," in *MICCAI*. Springer, 2021, pp. 451–460.
- [16] J. Wang, Y. Tang, Y. Xiao, J. T. Zhou, Z. Fang, and F. Yang, "Grenet: gradually recurrent network with curriculum learning for 2-d medical image segmentation," *IEEE Transactions on Neural Networks and Learning Systems*, 2023.
- [17] A. Wang, M. Islam, M. Xu, and H. Ren, "Curriculum-based augmented fourier domain adaptation for robust medical image segmentation," *IEEE Transactions on Automation Science and Engineering*, 2023.
- [18] F. Milletari, N. Navab, and S.-A. Ahmadi, "V-Net: Fully convolutional neural networks for volumetric medical image segmentation," in 3DV. Ieee, 2016, pp. 565–571.
- [19] C. Bauer, H. Bischof, and R. Beichel, "Segmentation of airways based on gradient vector flow," in *International workshop on pulmonary* image analysis, MICCAI, 2009, pp. 191–201.
- [20] P. Lo, B. Van Ginneken, J. M. Reinhardt, T. Yavarna, P. A. De Jong, B. Irving, C. Fetita, M. Ortner, R. Pinho, J. Sijbers, et al., "Extraction of airways from CT (EXACT'09)," *IEEE Transactions on Medical Imaging*, vol. 31, no. 11, pp. 2093–2107, 2012.

- [21] H. Zheng, Y. Qin, Y. Gu, F. Xie, J. Sun, J. Yang, and G.-Z. Yang, "Refined local-imbalance-based weight for airway segmentation in CT," in MICCAI. Springer, 2021, pp. 410–419.
- [22] C. Szegedy, W. Liu, Y. Jia, P. Sermanet, S. Reed, D. Anguelov, D. Erhan, V. Vanhoucke, and A. Rabinovich, "Going deeper with convolutions," in *Proceedings of the IEEE conference on computer* vision and pattern recognition, 2015, pp. 1–9.
- [23] M. Zhang, Y. Wu, H. Zhang, Y. Qin, H. Zheng, W. Tang, C. Arnold, C. Pei, P. Yu, Y. Nan, et al., "Multi-site, multi-domain airway tree modeling," Medical Image Analysis, vol. 90, p. 102957, 2023.
- [24] K. Palágyi, J. Tschirren, and M. Sonka, "Quantitative analysis of intrathoracic airway trees: methods and validation," in *IPMI*. Springer, 2003, pp. 222–233.
- [25] Z. Tan, J. Feng, and J. Zhou, "SGNet: Structure-aware graph-based network for airway semantic segmentation," in *MICCAI*. Springer, 2021, pp. 153–163.
- [26] J. Tschirren, G. McLennan, K. Palágyi, E. A. Hoffman, and M. Sonka, "Matching and anatomical labeling of human airway tree," *IEEE transactions on medical imaging*, vol. 24, no. 12, pp. 1540–1547, 2005.
- [27] W. Yu, H. Zheng, M. Zhang, H. Zhang, J. Sun, and J. Yang, "Break: Bronchi reconstruction by geodesic transformation and skeleton embedding," in *ISBI*. IEEE, 2022, pp. 1–5.
- [28] M. Zhang, H. Zhang, G.-Z. Yang, and Y. Gu, "CFDA: Collaborative feature disentanglement and augmentation for pulmonary airway tree modeling of COVID-19 CTs," in MICCAI. Springer, 2022, pp. 506– 516.
- [29] S. G. Armato III, G. McLennan, L. Bidaut, M. F. McNitt-Gray, C. R. Meyer, A. P. Reeves, B. Zhao, D. R. Aberle, C. I. Henschke, E. A. Hoffman, et al., "The lung image database consortium (LIDC) and image database resource initiative (IDRI): a completed reference database of lung nodules on CT scans," Medical physics, vol. 38, no. 2, pp. 915–931, 2011.
- [30] W. Liu, H. Yang, T. Tian, Z. Cao, X. Pan, W. Xu, Y. Jin, and F. Gao, "Full-resolution network and dual-threshold iteration for retinal vessel and coronary angiograph segmentation," *IEEE Journal of Biomedical* and Health Informatics, vol. 26, no. 9, pp. 4623–4634, 2022.
- [31] Y. Wu, S. Zhao, S. Qi, J. Feng, H. Pang, R. Chang, L. Bai, M. Li, S. Xia, W. Qian, et al., "Two-stage contextual transformer-based convolutional neural network for airway extraction from CT images," Artificial Intelligence in Medicine, vol. 143, p. 102637, 2023.
- [32] F. Isensee, P. F. Jaeger, S. A. Kohl, J. Petersen, and K. H. Maier-Hein, "nnU-Net: a self-configuring method for deep learning-based biomedical image segmentation," *Nature methods*, vol. 18, no. 2, pp. 203–211, 2021.
- [33] Y. Qin, H. Zheng, Y. Gu, X. Huang, J. Yang, L. Wang, F. Yao, Y.-M. Zhu, and G.-Z. Yang, "Learning tubule-sensitive CNNs for pulmonary airway and artery-vein segmentation in CT," *IEEE transactions on medical imaging*, vol. 40, no. 6, pp. 1603–1617, 2021.